

TextSSR: Diffusion-based Data Synthesis for Scene Text Recognition

Xingsong Ye, Yongkun Du, Yunbo Tao, Zhineng Chen*

School of Computer Science, Fudan University, China

{xsye20, zhincheng}@fudan.edu.cn, {ykdu23, ybtao24}@m.fudan.edu.cn

Abstract

Scene text recognition (STR) suffers from the challenges of either less realistic synthetic training data or the difficulty of collecting sufficient high-quality real-world data, limiting the effectiveness of trained STR models. Meanwhile, despite producing holistically appealing text images, diffusion-based text image generation methods struggle to generate accurate and realistic instance-level text on a large scale. To tackle this, we introduce **TextSSR**: a novel framework for **Synthesizing Scene Text Recognition** data via a diffusion-based universal text region synthesis model. It ensures accuracy by focusing on generating text within a specified image region and leveraging rich glyph and position information to create the less complex text region compared to the entire image. Furthermore, we utilize neighboring text within the region as a prompt to capture real-world font styles and layout patterns, guiding the generated text to resemble actual scenes. Finally, due to its prompt-free nature and capability for character-level synthesis, TextSSR enjoys a wonderful scalability and we construct an anagram-based TextSSR-F dataset with 0.4 million text instances with complexity and realism. Experiments show that models trained on added TextSSR-F data exhibit better accuracy compared to models trained on 4 million existing synthetic data. Moreover, its accuracy margin to models trained fully on a real-world dataset is less than 3.7%, confirming TextSSR’s effectiveness and its great potential in scene text image synthesis. Our code is available at <https://github.com/YesianRohn/TextSSR>.

1. Introduction

As a special kind of image captured in the wild, scene text images differ from general images in the presence of text, which appears with diverse layouts, fonts, and often with varying degrees of distortion and occlusion. However, the text usually contains high-level semantic information closely related to the captured scene, making scene text

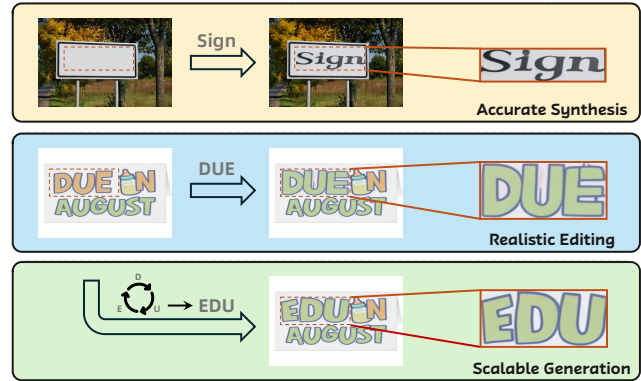


Figure 1. Showcases our method’s capacity to synthesize data by utilizing regional outputs inferred from the surrounding background or textual context alone.

recognition (STR) a crucial task for complex scene understanding, image search, etc.

Recent STR practices [11, 22] have shown that besides advanced modeling techniques, high-quality training data also plays a critical role in unleashing the model’s recognition capability. STR models trained based on diverse and rich real-world data [22] exhibit much higher accuracy compared to those trained based on typical synthetic datasets [16, 20]. Enlarging the size of real-world datasets is of course a practical way to further enhance recognition. However, it is challenging to collect real-world scene text images on an even larger scale. On one hand, diversified data collection is costly and time-consuming. On the other hand, real-world scenes predominantly contain high-frequency, semantically meaningful words, while low-frequency words are difficult to collect. Therefore, synthesizing high-quality text images seems to be an effective alternative. However, we note that MJ [20] and ST [16], the two most popular synthetic datasets, are constructed based on traditional rendering techniques nearly a decade ago. As illustrated in Fig. 3(a), although they can be easily scaled up in quantity, they suffer from limited diversity.

Recently, diffusion models have demonstrated significant potential in image editing and image generation, with

*Corresponding author.

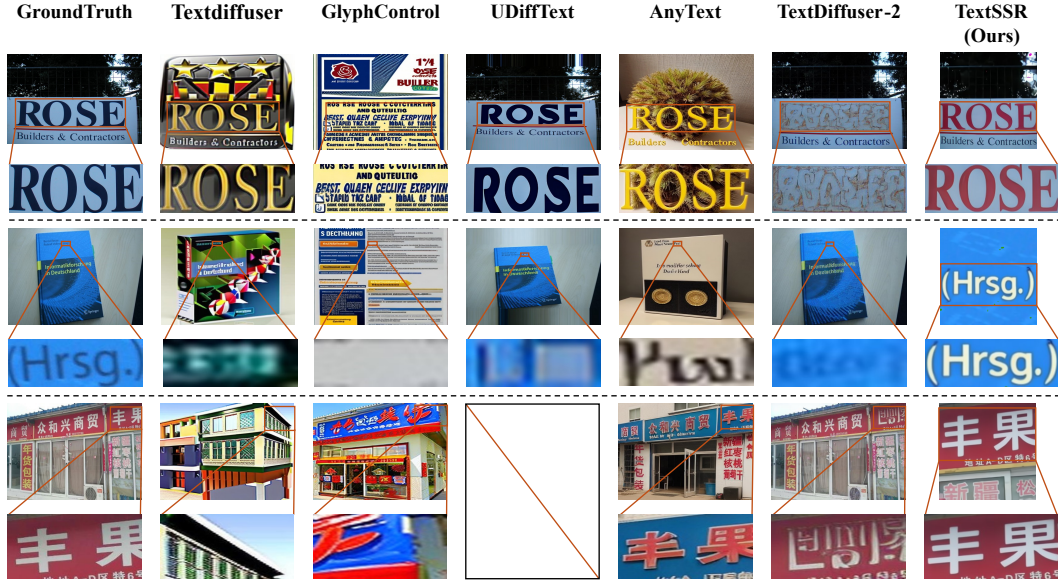


Figure 2. Examples synthesized by TextSSR and compare them with existing open-source methods (of which UDiffText only supports English). TextSSR reconstructs local images, whereas other methods operate on the entire image. Throughout the presentation, TextSSR consistently produces accurate and high-quality visual text. For further analysis, please refer to Appendix 7.1.

notable success in generating text-rich images [6, 7, 46, 53, 61]. However, most of the existing works (in Fig. 3(c)) focus on generating aesthetic text images holistically, e.g., posters. Using data generated by these methods for STR model training encounters several issues. First, these methods are designed for generation based on the entire image, when switching to synthesizing text in small-sized regions, it would be less effective and ensuring the generation accuracy becomes challenging. Second, current generation methods mainly rely on well-refined natural language as prompts, which tend to produce overly homogeneous and unrealistic images. Third, constructing a diverse set of prompts is inherently difficult, which hinders the ability to generate data on a large scale. Nevertheless, due to the exceptional performance of diffusion models in many tasks, we believe that qualified text instances can still be generated by appropriately handling the above issues.

Specifically, *to develop a better data synthesis method that can improve the training of STR models*, we summarize three key characteristics that such a method should exhibit:

- **Accurate:** It is essential that the synthesized text content should match the given text, ensuring that the synthesized words are readable and free from character misplacement or duplication errors. This is fundamental for maintaining the recognition model’s correctness.
- **Realistic:** The generated text regions should visually resemble real-world images, simulating realistic scene conditions. This includes perceiving the scales of text regions across the image to ensure consistent generation at differ-

ent sizes and capturing the diversity of text presentation, especially in complex scenes. Achieving realism is essential for enhancing the performance of text recognizers in the wild.

- **Scalable:** The method should support extensive training data production. It should minimize the need for complex control inputs and design processes, and enable large-scale data generation by leveraging easily accessible and processable texts or images. It would also be desirable to go beyond semantic or non-semantic text and also support the generation of arbitrary character sequences to enrich the dataset.

To deal with these challenges, we introduce a novel diffusion-based framework named **TextSSR**, which focuses on **Synthesizing Scene Text Recognition** data. To achieve greater accuracy in the generated content, TextSSR generates text within a specified region instead of the complex entire image, which often has an unknown text region size. Our position-glyph enhancement technique further resolves character duplication and positional disorder, ensuring precise text placement and arrangement. To ensure realistic results, we leverage the text near the designated region as contextual hints for font style and appearance, guiding the generated text to match real-world scenarios better. Notably, TextSSR operates without reliance on natural language prompts and requires only the specification of text position and the desired text content. Additionally, with the aid of rich character-level priors, it is capable of character-level rendering. These capabilities allow for large-scale

generation through random text permutations. This yields the TextSSR-F dataset with approximately 0.4 million new samples filtered through an STR model. Experimental results show that our synthesized data outperforms existing methods and approaches real-world data performance, particularly enhancing recognition on non-semantic words.

Our contributions can be summarized as follows:

- We propose TextSSR, a diffusion model-based text image synthesis method centered on text regions and invariant to scale. It is the first attempt at applying diffusion models to assist STR model training.
- TextSSR fully exploits positional and shape priors of text, achieving accurate, diverse and realistic instance-level text synthesis by using only textual inputs. Moreover, it can be easily scaled up and we construct the TextSSR-F dataset with 0.4 million text instances.
- Extensive evaluations validate the effectiveness of the models trained on TextSSR-F, which not only surpass models trained on much more other synthetic data, but also nearly match those trained on real-world data, highlighting the utility of the proposed TextSSR.

2. Related Work

2.1. Data Synthesis with Diffusion Models

Initial synthetic work advocates for the expansion of balanced datasets in zero-shot or few-shot scenarios [18, 38, 43]. Later works begin to explore the direct use of synthetic samples for training fundamental tasks such as image classification and recognition [1, 3], object detection [62] and semantic segmentation [31, 51]. Building on this, the application of diffusion models for synthetic data related to text has emerged, such as tabular data synthesis [26, 58], handwritten text synthesis [15, 32], and recently, some efforts have attempted scene text data synthesis from the perspectives of data augmentation and direct generation [63, 64].

2.2. Scene Text Recognition

The STR task typically involves performing sequence recognition on text regions detected by scene text detection. Compared to traditional optical character recognition (OCR) tasks, STR faces additional challenges, such as complex backgrounds, diverse text shapes, and occlusion or missing parts. Early approaches based on CNN-RNN-CTC [40, 55] methods use CNN for feature extraction, followed by RNN for sequence modeling, with CTC loss applied as a constraint. Subsequently, attention mechanisms gradually gain needed in the STR field [28, 39, 42]. Recently, inspired by developments in the NLP field, many methods [4, 13, 49] have further refined recognizers from a language modeling perspective. At the same time, some approaches [10, 60] continue to explore the potential of single-vision models without semantics. Unlike these model-

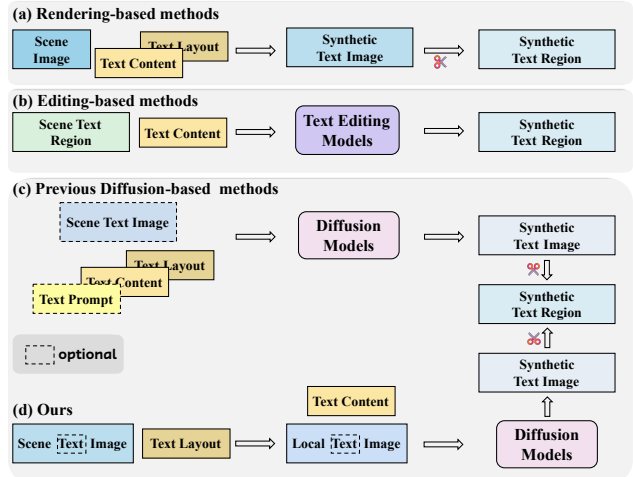


Figure 3. The pipeline comparison between TextSSR and previous methods. In (c), "optional" indicates that either or both options should be provided. And in (d), it means that the base image can be used with or without text.

improvement approaches, Union14M [22] points out current STR bottlenecks from a data perspective, so we also attempt to alleviate this challenge through synthetic data.

2.3. Scene Text Synthesis

Early text synthesis methods [16, 20, 27] rely on predefined rules to overlay text onto a target background, performing corresponding transformations and blending techniques to approximate real-world scenarios. To achieve more realistic scene text generation, subsequent research shifts toward deep learning-based generation methods. Among these, GAN-based scene text editing [34, 50, 52] methods, shown in Fig. 3(b), aim to enhance realism by generating text directly within specified regions. Nevertheless, a significant limitation of these approaches is the lack of real paired training data, as they are often trained on synthetic datasets, which restricts their applicability in real-world scenarios. More recent developments have employed diffusion models to unify both editing [19, 21, 54] and synthesis capabilities, enabling fine-grained control over glyph information [5, 53], word-level [46], and character-level [6, 61] positioning. Furthermore, the latest advancements [7, 64] incorporate (Multimodal) Large Language Models to further optimize performance.

3. Method

The overall framework of our proposed TextSSR method is illustrated in Fig. 4, with the training and inference processes of its generative model depicted in Fig. 5. In this work, we aim to focus on text regions and treat text instances of different scales fairly, which will be addressed in

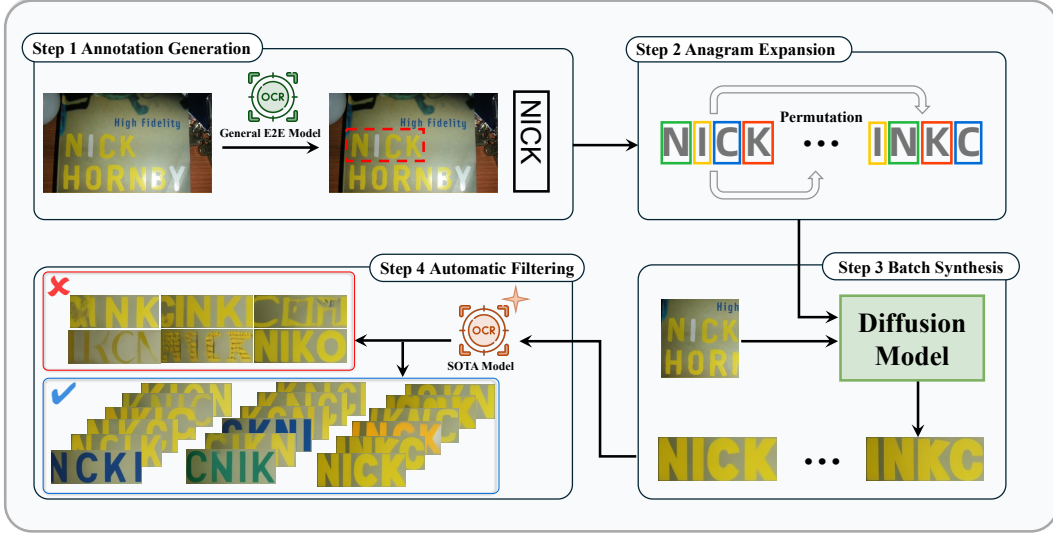


Figure 4. The large-scale data synthesis framework of TextSSR. A general end-to-end OCR model, such as PPOCRv3, extracts the text layout and content within the image (Step 1). All possible text words are generated through anagram (Step 2), then the generative model synthesizes text instances in batches (Step 3), and finally, a SOTA STR model (e.g., SVTRv2) filters the samples, retaining only the correct instances for use (Step 4). The accuracy of data synthesis in this batch can reach up to 75%, while also maintaining diversity in styles.

Sec. 3.1. To achieve fine-grained extraction and decoupling of text glyphs and positions for prior information, Sec. 3.2 and Sec. 3.3 will detail the specific module design and training strategy, respectively. Sec. 3.4 introduces our data extension method to generate dataset.

3.1. Text Region-Centric Processing

Synthesis method that relies on editing specified regions across the entire image is not suitable for text elements. It creates an imbalance and small text regions lack sufficient pixels for accurate reconstruction. This issue is particularly critical for text, where even slight inaccuracies in stroke generation can lead to significant semantic differences. Furthermore, information from the entire scene is often redundant for text region synthesis. For example, in Fig. 5, the text “kills” to be synthesized shares a similar style and context with the upper text and background, while the lower region is inconsistent in both content and appearance.

Therefore, we propose a self-supervised generative paradigm based on a locality assumption—*text styles are more likely to correlate with adjacent text and background information*. This method focuses the model on the text region, synthesizing it using only surrounding local context rather than the entire scene. Specifically, we use the annotated text box to extract the smallest enclosing square around the text region and resize it to a fixed size (e.g., 256). This approach also helps the model learn text synthesis directly from the background information, as local patches are more likely to contain only background compared to full images, where at least one text area is always present.

3.2. Fine-grained Condition Mechanisms

Text image rendering requires attention to two key fine-grained features: glyph structure and positional arrangement. These features can be considered at both the holistic (word-level) and individual (character-level) scales, as well as internal and external contexts. Holistic glyph structure pertains to the appearance of the entire word, while individual glyph structure focuses on each character. Similarly, the external refers to the location and orientation of the text region within the local image, whereas the internal pertains to the relative order of characters within a word. To guide the generative process, we incorporate the following features.

Word-level position and glyph guidance. Similar to editing models, we employ a binary mask (see Fig. 5(a)) to separate text from non-text regions, setting the text area to 0 and the rest to 1, which provides position information.

Additionally, word-level glyph rendering is performed by applying an affine transformation to place the rendered standard font word within the bounding rectangle of the text area (as shown in Fig. 5(a)), offering both glyph and placement guidance. *When we close the door on the original styled text, we must at least provide a simple window of this text at that location*. Previous research [5, 46, 53] has also established this step as a fundamental condition for embedding textual information.

Character-level position and glyph guidance. Holistic word-level information limits the model’s understanding to the word’s permutations of characters. This leads to confusion when synthesizing words composed of arbitrary characters, as we observe issues such as repeated or incorrect

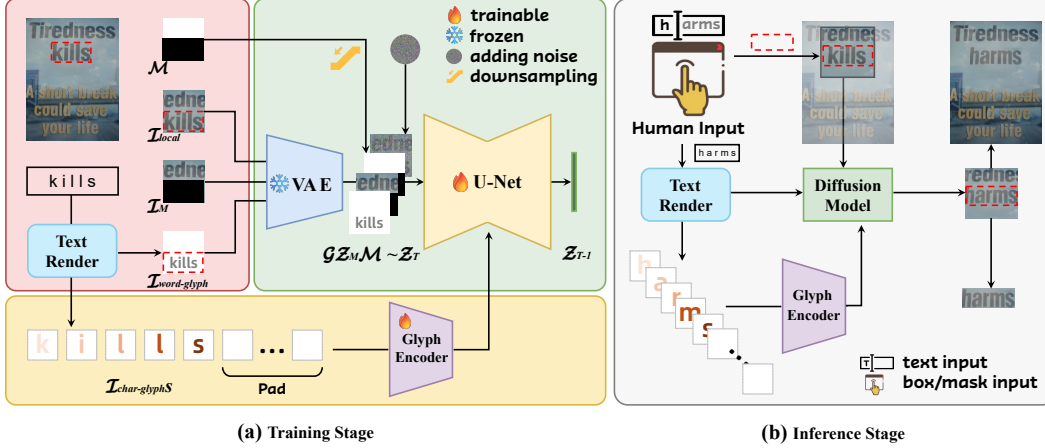


Figure 5. Overall architecture of the TextSSR’s generative model. (a) Given a scene text image annotated with a text box (marked in red) and text content (e.g., “kills”), it is preprocessed into the smallest local image containing a text region. (b) Text rendering can be performed in existing regions using either available annotations or user input to complete the generation task.

characters when using only word-level features. We introduce character-level ordering as a position prior encoded through pixel values, allowing the model to learn the spatial relationships between characters. Specifically, for characters from position 1 to L , the i -th character is rendered into the i -th channel of an L -channel image. The glyph for each character is rendered with a pixel value of $i \times \lfloor \frac{P_M}{L} \rfloor$ pixels, where P_M denotes the maximum number of pixels allocated for distinguishing a character from the background.

We employ Vision Transformer (ViT) [9] as the Glyph Encoder G_ϕ for accommodating input glyphs with L -channel and to output dimensions compatible with diffusion model inputs. The input is represented as a tensor $\mathbf{X} \in \mathbb{R}^{L \times S \times S}$, where S indicates the size of each glyph image. So the output features F_g can thus be represented as:

$$F_g = G_\phi(\mathbf{X}) \in \mathbb{R}^{(N+1) \times D}. \quad (1)$$

Here, N represents the number of patches, the additional one corresponds to a class token, and dimension D is set to match the input requirements of the diffusion process.

3.3. Fine-tune the Stable Diffusion

We leverage a pretrained model and fine-tune both its Variational Auto Encoder (VAE) and Conditional Diffusion Model (CDM) components for our specific task.

VAE Fine-tuning. The standard VAE, when pretrained on general datasets, may not be sensitive enough to capture the fine-grained spatial and glyph features of scaled text instances. As highlighted by DiffUTE [5] and confirmed by our ablation experiment 5, fine-tuning the VAE is essential when working with text images. Thus, we try it to enhance its capacity for accurate representation of text regions

in a fair, local manner, and its necessity is further validated through our ablation studies. The VAE consists of an encoder E_θ and a decoder D_θ , and we let V_θ represent the reconstruction after the encoding and decoding process. If x is a local image patch input, we aim to minimize the following loss function:

$$\mathcal{L}_{\text{TextSSR-VAE}} = \|V_\theta(x) - x\|_2^2. \quad (2)$$

CDM Training Process. We begin by processing a square local image I_{local} derived from Sec. 3.1. Then, we recalculate the text layout position and generate the corresponding mask M (will be downsampled) for the text area according to Sec. 3.2 and overlay it on the original image to generate the mask image I_M . At the same time, the word-level glyphs $I_{\text{word-glyph}}$ and individual character images $I_{\text{char-glyphs}}$ can also be obtained. The specific illustration for each one can be found in Fig. 5.

I_M , $I_{\text{word-glyph}}$, and I_{local} are fed into our VAE, generating latent representations Z_M and G . Additionally, I_{local} is further processed with added noise to produce Z_T . These latent features, concatenated with the resized positional mask M , serve as inputs to the CDM. Meanwhile, Proc. 1 provides fine-grained control conditions F_g . Finally, the CDM processes these inputs and produces the denoised latent representation Z_{T-1} , progressively refining the noisy input to recover the clean latent space. The model is trained by minimizing the following objective:

$$\mathcal{L}_{\text{TextSSR-CDM}} = \|\epsilon - \epsilon_\theta(z_t, t, Z_M, G, M, F_g)\|_2^2. \quad (3)$$

3.4. Large-scale Generation with Anagram

Our generation strategy begins by using the text layout and detected text from an OCR engine as inputs to our model.

| Method | ICDAR13 [23] | | | ICDAR15 [24] | | | ShopSign [57] | | |
|--------------------|----------------------|----------------|--------------------|----------------------|----------------|--------------------|----------------------|----------------|--------------------|
| | SeqAcc(%) \uparrow | NED \uparrow | FID-R \downarrow | SeqAcc(%) \uparrow | NED \uparrow | FID-R \downarrow | SeqAcc(%) \uparrow | NED \uparrow | FID-R \downarrow |
| TextDiffuser [6] | 25.08 | 0.4779 | 103.74 | 0.82 | 0.0551 | 120.66 | 0.64 | 0.0230 | 136.56 |
| GlyphControl [53] | 0.55 | 0.0472 | 142.91 | 0 | 0.0217 | 152.37 | 0 | 0.0067 | 140.91 |
| UDiffText [61] | 37.51 | 0.5892 | 67.82 | 2.55 | 0.1206 | 103.43 | — | — | — |
| AnyText [46] | 55.07 | 0.7153 | 75.46 | 5.97 | 0.2186 | 76.03 | 33.58 | 0.4602 | 89.25 |
| TextDiffuser-2 [7] | 26.39 | 0.5342 | 68.31 | 0.87 | 0.0838 | 82.93 | 0.82 | 0.0411 | 101.46 |
| TextSSR-Step1 | 75.35 | 0.9007 | 51.75 | 50.46 | 0.7361 | 34.69 | 30.28 | 0.5075 | 54.24 |
| TextSSR-Step2 | 85.17 | 0.9402 | 53.28 | 62.64 | 0.8087 | 36.30 | 52.24 | 0.7053 | 52.84 |
| Real | 96.51 | 0.9895 | 0 | 84.88 | 0.9486 | 0 | 74.84 | 0.8699 | 0 |

Table 1. Comparing of TextSSR (including two-step training results) and existing synthesis methods on regular text (ICDAR2013), difficult irregular text (ICDAR2015), and Multi-Language text (ShopSign) datasets, alongside results from real datasets (Real). SeqAcc and NED denote the recognition accuracy, editing distance, respectively. FID-R score means using the original text region to assess FID.

Since the original text content is masked during generation, any inaccuracies in OCR detection are hard to affect the rendered outcome. This process produces as many synthesized text regions as there are pseudo-labels. By keeping the background constant and varying only the synthesized text content, we can significantly expand the dataset. Unlike prior methods [6, 61] that simply select text strings of equal length for editing, our approach ensures a better correspondence between the text region and the content by changing the internal order. This is because there is a strong correspondence between text layout and text content (e.g., variations in character size and text length need to be considered). As shown in Fig. 5(b), to perfectly render visual text matching the word “harms”, it is necessary to adjust the text box to fit accordingly.

Recognizing text requires not only classifying individual characters but also understanding character relationships within sequences. We have also observed that most of the samples in the current dataset consist of semantic words, whereas there is a demand for non-semantic scene text data, such as store names and phone numbers. Therefore, our goal is to increase the diversity of text sequences and the presence of non-semantic words. Since our method utilizes character-level information to generate text with non-semantic content, we can shuffle the positions of characters within a word, allowing us to perform an “anagram-like” operation to generate a large number of diverse data samples. Given a word of length L , the number of possible permutations is

$$A_L^L = L!. \quad (4)$$

If we have 1k words of average length 10, the number of possible permutations would be approximately $10^3 \times 10!$, or around 3.6 billion samples. This volume of data is sufficient for robust training.

4. Experiments

Implementation details can be found in Appendix 6. Please note that our filtering rules only apply to the final large-scale

data generation phase (Tab. 4). For evaluating the generative model, we will directly use all generated data.

4.1. Benchmark and Evaluation Metrics

We propose comprehensive benchmarks that evaluate both accuracy and visual quality, while also assessing the ability of our synthetic dataset on larger scales.

Accuracy Evaluation. Evaluating the accuracy of generated scene text is challenging, as manually verifying alignment with target text is costly and inefficient. Therefore, previous benchmarks typically employ an STR model to automatically assess text consistency. However, this method can lead to incorrect conclusions, as the OCR model may misidentify synthetically generated data that is otherwise useful for improving recognition performance. To more effectively reflect the accuracy and difficulty level of our synthetic data, we have kept abreast of the times by choosing the current SOTA STR model, SVTRv2 [12], an open-source model released by PaddleOCR.

From Tab. 1, these results highlight TextSSR’s superior performance across datasets of varying difficulty and linguistic diversity. This contributes to the substantial performance gap observed between our results and theirs. TextSSR treats text regions fairly without such filtering, yielding notably better outcomes on small-sized test samples, thereby outperforming the current SOTA by 30.1% in overall accuracy. Moreover, methods based on whole-image synthesis struggle significantly in complex, challenging scenarios, as demonstrated by catastrophic results on the IC15 dataset. This dataset includes numerous small-sized text instances, a challenge that previous methods fail to address effectively. In contrast, TextSSR benefits from a region-centered generation paradigm that excels in handling small-sized text instances, maintaining high synthesis accuracy even in such difficult conditions. Furthermore, the ShopSign dataset results underscore TextSSR’s multilingual capability, outperforming the purportedly multilingual-focused Anytext by 18.39%.

| Method | Benchmark SeqAcc(%) | | |
|---------------------|---------------------|--------------|--------------|
| | Regular | Irregular | Avg |
| SynthText† [16] | 48.55 | 26.08 | 39.74 |
| VISD† [56] | 38.02 | 26.88 | 33.65 |
| UnrealText† [27] | 32.06 | 19.85 | 27.28 |
| TextDiffuser† [6] | 30.08 | 8.79 | 21.74 |
| GlyphControl† [53] | 40.80 | 13.21 | 29.99 |
| AnyText† [46] | 49.80 | 19.62 | 37.97 |
| TextDiffuser-2† [7] | 40.26 | 10.48 | 28.59 |
| SceneVTG† [64] | 54.97 | 35.50 | 47.34 |
| SceneVTG-Real† | <u>57.97</u> | 37.66 | 50.01 |
| TextSSR (Ours) | 59.76 | 35.71 | 50.33 |
| TextOCR-Real [44] | 57.83 | <u>41.56</u> | <u>54.05</u> |

Table 2. Comparison of the effects of training CRNN [40] on different synthetic data and real data [2] of 30k order of magnitude. “Regular” denotes the average performance on IIIT [29], SVT [48], and IC13 [23] datasets, “Irregular” represents the results across IC15 [24], SVTP [33], and CUTE [35] datasets, while “Avg” is the average performance from these datasets. † means data borrowed from SceneVTG [64]; the setup of the additional experiments is also consistent with it.

Realism Evaluation. Following the methodology presented in SceneVTG [64], we generate a fixed amount of data to train an identical model under fair and identical settings and then test it on common text recognition benchmarks. This approach avoids the need for separate verification of text correctness or synthesis quality; if the generated text is inaccurate or unrealistic, this will be reflected in poor recognition performance during testing. As shown in Tab. 2, aside from Anytext, the diffusion-based methods from the previous experiment perform significantly worse than rendering-based synthetic data, which is closely linked to their low text accuracy. SceneVTG benefits from its two-stage pipeline of text erasure followed by rendering to achieve outstanding results. In contrast, TextSSR, following the mask-based paradigm like Anytext without text erasure, still surpasses SceneVTG by 2.99%. By leveraging the more challenging TextOCR dataset as a foundation, we achieve results exceeding those reported on real data in SceneVTG, demonstrating the robustness and adaptability of our approach.

Scalability Evaluation. To examine whether our scalable method improves STR model performance, we apply to expand the training dataset by 2x, 4x, and 8x, which (refer to Tab. 3) is also an additional experiment for Exp. 2. The results show that as the data volume gradually doubles, performance improves incrementally by -0.04%, 4.7%, and 14.11%, eventually surpassing the performance of using real and pseudo-labeled data. This outcome demonstrates the scalability and effectiveness of our synthesis approach which significantly benefits STR model training.

| Method | Size | Benchmark SeqAcc(%) | | |
|-----------------|------|---------------------|--------------|--------------|
| | | Regular | Irregular | Avg |
| TextSSR x1 | 30k | 59.76 | 35.71 | 50.33 |
| TextSSR EL-Edit | 30k | 24.58 | 10.23 | 18.95 |
| TextSSR Anagram | 30k | 51.41 | 28.90 | 42.86 |
| TextSSR x2 | 60k | 60.49 | 34.49 | 50.29 |
| TextSSR x4 | 120k | 65.17 | 39.34 | 55.03 |
| TextSSR x8 | 240k | 73.96 | 49.69 | 64.44 |
| TextOCR Real | 30k | 57.83 | 41.56 | 54.05 |
| TextOCR Pseudo | 30k | 69.78 | 45.98 | 60.44 |

Table 3. Results for TextSSR data augmentation, x1 refers to rendering directly with given labels, while EL-Edit edits text of equal length (EL). When expanded to n times, we combine x1 results with (n-1) times of data synthesized via the Anagram method.

Usability Assessment. In addition, we assess the effectiveness of our synthesis method in supporting the large-scale training of STR models. The training results from various data sources in the Tab. 4 can be analyzed as follows: (1) When incorporating our synthetic dataset, the average performance across three STR models improved by 2.93% over the 4 million-sample ST dataset, also outperforming the full ST dataset by 2.77% and coming within just 0.22% of real data performance. This suggests that the filtered TextSSR-F dataset achieves near-realistic authenticity while maintaining high accuracy. (2) Due to the inherently semantic-free generation capability of our extended method, performance on the “Contextless” benchmark—a semantic-free evaluation standard—exceeds that of the real dataset by 8.47%, underscoring the robustness of our approach in non-semantic contexts.

4.2. Ablation Study

We start with the base model configuration and incrementally add each component or method. Then, we individually remove them from the final configuration to assess their respective necessity and effectiveness. From the results on Tab. 5, we can see that the removal of each one brings about a decline in effectiveness, while the absence of “Region-Centric” processing leads to a catastrophic drop of 35.44% in accuracy.

The results in Fig. 6 show that traditional methods, which handle the text region across the entire image, exhibit a performance trend that rises and then falls as the size increases. This is due to the fact that when the region is small, the entire image is scaled, resulting in more blurred text regions and insufficient pixels for text rendering. As the region size increases, the amount of text content also grows, causing the accuracy to decline. In contrast, incorporating Region-Centric processing allows TextSSR to achieve superior and consistent performance across all sizes. Fig. 7 il-

| Model | Dataset | Size | Benchmark SeqAcc(%) | | | | | | | |
|-------------|--------------|----------|---------------------|--------------|--------------|--------------|--------------|--------------|--------------|------------------|
| | | | IIIT5k [29] | SVT [48] | IC13 [23] | IC15 [24] | SVTP [33] | CUTE80 [35] | Avg | Contextless [22] |
| CRNN [40] | ST | 400w | 90.20 | 83.62 | 91.20 | 72.94 | 72.71 | 77.78 | 81.24 | 29.65 |
| | TextSSR-F+ST | 43w+400w | 92.37 | 87.79 | 92.65 | 76.86 | 75.35 | 81.94 | 84.49 | 51.99 |
| | TextOCR+ST | 43w+400w | 91.23 | 86.09 | 91.72 | 77.31 | 73.95 | 81.60 | 83.65 | 39.79 |
| | ST | 698w | 89.53 | 81.30 | 91.95 | 72.56 | 71.01 | 75.35 | 80.28 | 31.58 |
| NRTR [39] | ST | 400w | 93.90 | 89.03 | 95.10 | 80.18 | 80.93 | 81.25 | 86.73 | 38.13 |
| | TextSSR-F+ST | 43w+400w | 96.10 | 91.96 | 96.15 | 84.65 | 84.03 | 86.81 | 89.95 | 60.33 |
| | TextOCR+ST | 43w+400w | 95.97 | 93.35 | 95.80 | 86.31 | 85.58 | 88.54 | 90.92 | 55.20 |
| | ST | 698w | 93.60 | 90.11 | 95.10 | 81.23 | 82.33 | 84.03 | 87.73 | 43.00 |
| ABINet [13] | ST | 400w | 92.00 | 87.17 | 93.35 | 77.31 | 77.05 | 87.50 | 85.73 | 42.49 |
| | TextSSR-F+ST | 43w+400w | 94.80 | 90.57 | 94.05 | 80.89 | 80.78 | 87.15 | 88.04 | 62.90 |
| | TextOCR+ST | 43w+400w | 94.63 | 91.19 | 92.99 | 82.88 | 81.55 | 90.28 | 88.92 | 54.81 |
| | ST | 698w | 93.63 | 87.02 | 93.23 | 77.25 | 79.38 | 86.46 | 86.16 | 45.06 |

Table 4. Training on three representative models using datasets from three different sources for large-scale text recognition, and then evaluating the results on the STR Benchmark.

| Region-Centric | Char-Glyph | Char-Position | Fine-tune VAE | SeqAcc (%) \uparrow | NED \uparrow | FID-R \downarrow |
|----------------|--------------|---------------|---------------|-----------------------|----------------|--------------------|
| \times | \times | \times | \times | 20.28 | 0.3444 | 102.89 |
| \checkmark | \times | \times | \times | 73.50 | 0.8764 | 45.89 |
| \checkmark | \checkmark | \times | \times | 74.15 | 0.8852 | 46.65 |
| \checkmark | \checkmark | \checkmark | \times | 80.26 | 0.9133 | 45.83 |
| \checkmark | \checkmark | \times | \checkmark | 77.21 | 0.9043 | 50.34 |
| \checkmark | \times | \times | \checkmark | 76.23 | 0.8991 | 51.94 |
| \times | \checkmark | \checkmark | \checkmark | 47.55 | 0.6211 | 62.52 |
| \checkmark | \checkmark | \checkmark | \checkmark | 82.99 | 0.9308 | 50.76 |

Table 5. Ablation study of the TextSSR model, adapting the step-1 pretrained model for fine-tuning on the AnyWord-Scene dataset. The results on the ICDAR2013 benchmark confirm the effectiveness of each processing step and submodule.

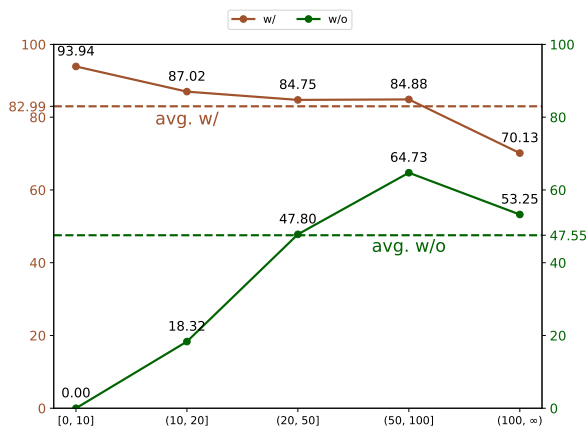


Figure 6. Performance of TextSSR with and without Region-Centric processing across text regions of different sizes. The horizontal axis represents the range of the minimum side length of the text region, while the vertical axis indicates the SeqAcc.

illustrates the impact of character-level position and glyph on the rendering results of TextSSR. The results indicate that omitting either component leads to issues such as character deformation, incorrect characters, and duplication errors in some cases. Additionally, fine-tuning the VAE offers a trade-off, slightly sacrificing visual quality for an improvement in accuracy.



Figure 7. Visualization results of TextSSR with and without character-level prior information. Further show details are provided in Appendix 7.3

5. Conclusion

With in mind that current diffusion-based methods are insufficient to generate high-quality scene text instances for STR model training, we have proposed TextSSR. By employing the surrounding context as the prompt and imposing character-level constraints, TextSSR can generate accurate and realistic text instances at a large scale. We have constructed the TextSSR-F dataset with 0.4 million diverse and realistic instances. Then, we have evaluated models trained respectively on TextSSR-F, traditional synthetic data, and real-world TextOCR.

TextSSR-F-trained models show obvious advantages compared to those trained on existing synthetic data, highlighting the effectiveness of TextSSR. However, although outperforming TextOCR's results in regular text, there is still a gap between TextSSR and TextOCR in irregular text. Thus, future work includes the exploration of more controllable ways to further improve the generation quality. We are also interested in extending TextSSR to generate text in different languages like Chinese.

References

- [1] S. Azizi, S. Kornblith, C. Saharia, M. Norouzi, and D.J. Fleet. Synthetic data from diffusion models improves imagenet classification. *TMLR*, 2024. 3
- [2] J. Baek, Y. Matsui, and K. Aizawa. What if we only use real datasets for scene text recognition? toward scene text recognition with fewer labels. In *CVPR*, 2021. 7, 2
- [3] H. Bansal and A. Grover. Leaving reality to imagination: Robust classification via generated datasets. *arXiv preprint arXiv:2302.02503*, 2023. 3
- [4] D. Bautista and R. Atienza. Scene text recognition with permuted autoregressive sequence models. In *ECCV*, 2022. 3
- [5] H. Chen, Z. Xu, Z. Gu, J. Lan, X. Zheng, Y. Li, C. Meng, H. Zhu, and W. Wang. DIFFUTE: Universal text editing diffusion model. In *NIPS*, 2023. 3, 4, 5
- [6] J. Chen, Y. Huang, T. Lv, L. Cui, Q. Chen, and F. Wei. TextDiffuser: Diffusion models as text painters. In *NIPS*, 2023. 2, 3, 6, 7
- [7] J. Chen, Y. Huang, T. Lv, L. Cui, Q. Chen, and F. Wei. Textdiffuser-2: Unleashing the power of language models for text rendering. In *ECCV*, 2024. 2, 3, 6, 7
- [8] C.K. Chng, Y. Liu, Y. Sun, C.C. Ng, C. Luo, Z. Ni, C.M. Fang, S. Zhang, J. Han, E. Ding, J. Liu, D. Karatzas, C.S. Chan, and L. Jin. ICDAR2019 robust reading challenge on arbitrary-shaped text - rrc-art. In *ICDAR*, 2019. 1
- [9] A. Dosovitskiy, L. Beyer, A. Kolesnikov, D. Weissenborn, X. Zhai, T. Unterthiner, M. Dehghani, M. Minderer, G. Heigold, S. Gelly, J. Uszkoreit, and N. Houlsby. An image is worth 16x16 words: Transformers for image recognition at scale. In *ICLR*, 2021. 5
- [10] Y. Du, Z. Chen, C. Jia, X. Yin, T. Zheng, C. Li, Y. Du, and Y. Jiang. SVTR: Scene text recognition with a single visual model. In *IJCAI*, 2022. 3
- [11] Y. Du, Z. Chen, C. Jia, X. Yin, C. Li, Y. Du, and Y. Jiang. Context perception parallel decoder for scene text recognition. *arXiv preprint arXiv:2307.12270*, 2023. 1
- [12] Y. Du, Z. Chen, H. Xie, C. Jia, and Y. Jiang. Svtrv2: Ctc beats encoder-decoder models in scene text recognition. *arXiv preprint arXiv:2411.15858*, 2024. 6
- [13] S. Fang, H. Xie, Y. Wang, Z. Mao, and Y. Zhang. Read like humans: Autonomous, bidirectional and iterative language modeling for scene text recognition. In *CVPR*, 2021. 3, 8, 2
- [14] J. Gu, X. Meng, G. Lu, L. Hou, N. Minzhe, X. Liang, L. Yao, R. Huang, W. Zhang, X. Jiang, C. Xu, and H. Xu. Wukong: A 100 million large-scale chinese cross-modal pre-training benchmark. In *NIPS*, 2022. 1
- [15] D. Gui, K. Chen, H. Ding, and Q. Huo. Zero-shot generation of training data with denoising diffusion probabilistic model for handwritten chinese character recognition. In *ICDAR*, 2023. 3
- [16] A. Gupta, A. Vedaldi, and A. Zisserman. Synthetic data for text localisation in natural images. In *CVPR*, 2016. 1, 3, 7
- [17] M. He, Y. Liu, Z. Yang, S. Zhang, C. Luo, F. Gao, Q. Zheng, Y. Wang, X. Zhang, and L. Jin. ICPR2018 contest on robust reading for multi-type web images. In *ICPR*, 2018. 1
- [18] R. He, S. Sun, X. Yu, C. Xue, W. Zhang, P.H.S. Torr, S. Bai, and X. Qi. Is synthetic data from generative models ready for image recognition? In *ICLR*, 2023. 3
- [19] Santoso J, Simon C, and Williemi. On manipulating scene text in the wild with diffusion models. In *WACV*, 2024. 3
- [20] M. Jaderberg, K. Simonyan, A. Vedaldi, and A. Zisserman. Synthetic data and artificial neural networks for natural scene text recognition. In *Workshop on Deep Learning, NIPS*, 2014. 1, 3
- [21] J. Ji, G. Zhang, Z. Wang, B. Hou, Z. Zhang, B. Price, and S. Chang. Improving diffusion models for scene text editing with dual encoders. *TMLR*, 2024. 3
- [22] Q. Jiang, J. Wang, D. Peng, C. Liu, and L. Jin. Revisiting scene text recognition: A data perspective. In *ICCV*, 2023. 1, 3, 8
- [23] D. Karatzas, F. Shafait, S. Uchida, M. Iwamura, L. Gomez i Bigorda, S. Robles Mestre, J. Mas, D. Fernandez Mota, J. Almazàn, and L.P. de las Heras. ICDAR 2013 robust reading competition. In *ICDAR*, 2013. 6, 7, 8, 1
- [24] D. Karatzas, L. Gomez-Bigorda, A. Nicolaou, S. Ghosh, A. Bagdanov, M. Iwamura, J. Matas, L. Neumann, V.R. Chandrasekhar, S. Lu, F. Shafait, S. Uchida, and E. Valveny. IC-DAR 2015 competition on robust reading. In *ICDAR*, 2015. 6, 7, 8, 1
- [25] C. Li, W. Liu, R. Guo, X. Yin, K. Jiang, Y. Du, Y. Du, L. Zhu, B. Lai, X. Hu, D. Yu, and Y. Ma. PP-OCRv3: More attempts for the improvement of ultra lightweight ocr system. *arXiv preprint arXiv:2206.03001*, 2022. 1
- [26] T. Liu, J. Fan, N. Tang, G. Li, and X. Du. Controllable tabular data synthesis using diffusion models. *PACMMOD*, 2024. 3
- [27] S. Long and C. Yao. Unrealtext: Synthesizing realistic scene text images from the unreal world. In *CVPR*, 2020. 3, 7
- [28] C. Luo, L. Jin, and Z. Sun. Moran: A multi-object rectified attention network for scene text recognition. *PR*, 2019. 3
- [29] A. Mishra, K. Alahari, and CV Jawahar. Scene text recognition using higher order language priors. In *BMVC*, 2012. 7, 8
- [30] N. Nayef, C. Liu, J. Ogier, Y. Patel, M. Busta, P.N. Chowdhury, D. Karatzas, W. Khlif, J. Matas, U. Pal, and J. Burie. ICDAR2019 robust reading challenge on multi-lingual scene text detection and recognition - rrc-mlt-2019. In *ICDAR*, 2019. 1
- [31] Q. Nguyen, T. Vu, A. Tran, and K. Nguyen. Dataset diffusion: Diffusion-based synthetic data generation for pixel-level semantic segmentation. In *NIPS*, 2024. 3
- [32] K. Nikolaidou, G. Retsinas, V. Christlein, M. Seuret, G. Sfikas, E.B. Smith, H. Mokayed, and M. Liwicki. Wordstylist: styled verbatim handwritten text generation with latent diffusion models. In *ICDAR*, 2023. 3

- [33] T. Q. Phan, P. Shivakumara, S. Tian, and C. L. Tan. Recognizing text with perspective distortion in natural scenes. In *ICCV*, 2013. 7, 8
- [34] Y. Qu, Q. Tan, H. Xie, J. Xu, Y. Wang, and Y. Zhang. Exploring stroke-level modifications for scene text editing. In *AAAI*, 2023. 3
- [35] A. Risnumawan, P. Shivakumara, C. S. Chan, and C. L. Tan. A robust arbitrary text detection system for natural scene images. *ESWA*, 2014. 7, 8
- [36] R. Rombach, A. Blattmann, D. Lorenz, P. Esser, and B. Ommer. High-resolution image synthesis with latent diffusion models. In *CVPR*, 2022. 1
- [37] C. Schuhmann, R. Vencu, R. Beaumont, R. Kaczmarczyk, C. Mullis, A. Katta, T. Coombes, J. Jitsev, and A. Komatsuzaki. Laion-400m: Open dataset of clip-filtered 400 million image-text pairs. *arXiv preprint arXiv:2111.02114*, 2021. 1
- [38] V. Schwag, C. Hazirbas, A. Gordo, F. Ozgenel, and C. Canton. Generating high fidelity data from low-density regions using diffusion models. In *CVPR*, 2022. 3
- [39] F. Sheng, Z. Chen, and B. Xu. NRTR: A no-recurrence sequence-to-sequence model for scene text recognition. In *ICDAR*, 2019. 3, 8, 2
- [40] B. Shi, X. Bai, and C. Yao. An end-to-end trainable neural network for image-based sequence recognition and its application to scene text recognition. *TPAMI*, 2016. 3, 7, 8, 2
- [41] B. Shi, C. Yao, M. Liao, M. Yang, P. Xu, L. Cui, S. Belongie, S. Lu, and X. Bai. ICDAR2017 competition on reading chinese text in the wild (rctw-17). In *ICDAR*, 2017. 1
- [42] B. Shi, M. Yang, X. Wang, P. Lyu, C. Yao, and X. Bai. Aster: An attentional scene text recognizer with flexible rectification. *TPAMI*, 2018. 3
- [43] J. Shipard, A. Wiliem, K. N. Thanh, W. Xiang, and C. Fookes. Diversity is definitely needed: Improving model-agnostic zero-shot classification via stable diffusion. In *CVPR*, 2023. 3
- [44] A. Singh, G. Pang, M. Toh, J. Huang, W. Galuba, and T. Hassner. Textocr: Towards large-scale end-to-end reasoning for arbitrary-shaped scene text. In *CVPR*, 2021. 7, 1
- [45] Y. Sun, Z. Ni, C.K. Chng, Y. Liu, C. Luo, C.C. Ng, J. Han, E. Ding, J. Liu, D. Karatzas, C.S. Chan, and L. Jin. ICDAR 2019 competition on large-scale street view text with partial labeling-rrc-lsvt. In *ICDAR*, 2019. 1
- [46] Y. Tuo, W. Xiang, J. Y. He, Y. Geng, and X. Xie. AnyText: Multilingual visual text generation and editing. In *ICLR*, 2024. 2, 3, 4, 6, 7, 1
- [47] A. Veit, T. Matera, L. Neumann, J. Matas, and S. Belongie. Coco-text: Dataset and benchmark for text detection and recognition in natural images. *arXiv preprint arXiv:1601.07140*, 2016. 1
- [48] K. Wang, B. Babenko, and S. Belongie. End-to-end scene text recognition. In *ICCV*, 2011. 7, 8
- [49] J. Wei, H. Zhan, Y. Lu, X. Tu, B. Yin, C. Liu, and U. Pal. Image as a language: Revisiting scene text recognition via balanced, unified and synchronized vision-language reasoning network. In *AAAI*, 2024. 3
- [50] L. Wu, C. Zhang, J. Liu, J. Han, J. Liu, E. Ding, and X. Bai. Editing text in the wild. In *ACMMM*, 2019. 3
- [51] W. Wu, Y. Zhao, H. Chen, Y. Gu, R. Zhao, Y. He, H. Zhou, M.Z. Shou, and C. Shen. Datasetdm: Synthesizing data with perception annotations using diffusion models. In *NIPS*, 2023. 3
- [52] Q. Yang, J. Huang, and W. Lin. Swaptxt: Image based texts transfer in scenes. In *CVPR*, 2020. 3
- [53] Y. Yang, D. Gui, Y. Yuan, W. Liang, H. Ding, H. Hu, and K. Chen. GlyphControl: Glyph conditional control for visual text generation. In *NIPS*, 2023. 2, 3, 4, 6, 7
- [54] W. Zeng, Y. Shu, Z. Li, D. Yang, and Y. Zhou. TextCtrl: Diffusion-based scene text editing with prior guidance control. In *NIPS*, 2024. 3
- [55] C. Zhai, Z. Chen, J. Li, and B. Xu. Chinese image text recognition with blstm-ctc: a segmentation-free method. In *PR*, 2016. 3
- [56] F. Zhan, S. Lu, and C. Xue. Verisimilar image synthesis for accurate detection and recognition of texts in scenes. In *ECCV*, 2018. 7
- [57] C. Zhang, W. Ding, G. Peng, F. Fu, and W. Wang. Street view text recognition with deep learning for urban scene understanding in intelligent transportation systems. *TITS*, 2021. 6, 1
- [58] H. Zhang, J. Zhang, B. Srinivasan, Z. Shen, X. Qin, C. Faloutsos, H. Rangwala, and G. Karypis. Mixed-type tabular data synthesis with score-based diffusion in latent space. In *ICLR*, 2024. 3
- [59] R. Zhang, Y. Zhou, Q. Jiang, Q. Song, N. Li, K. Zhou, L. Wang, D. Wang, M. Liao, M. Yang, X. Bai, B. Shi, D. Karatzas, S. Lu, and C.V. Jawahar. ICDAR 2019 robust reading challenge on reading chinese text on signboard. In *ICDAR*, 2019. 1
- [60] Z. Zhang, N. Lu, M. Liao, Y. Huang, C. Li, M. Wang, and W. Peng. Self-distillation regularized connectionist temporal classification loss for text recognition: A simple yet effective approach. In *AAAI*, 2024. 3
- [61] Y. Zhao and Z. Lian. UDiffText: A unified framework for high-quality text synthesis in arbitrary images via character-aware diffusion models. In *ECCV*, 2024. 2, 3, 6
- [62] J. Zhu, S. Li, Y. Liu, P. Huang, J. Shan, H. Ma, and J. Yuan. ODGEN: Domain-specific object detection data generation with diffusion models. In *NIPS*, 2024. 3
- [63] Y. Zhu, Z. Li, T. Wang, M. He, and C. Yao. Conditional text image generation with diffusion models. In *CVPR*, 2023. 3
- [64] Y. Zhu, J. Liu, F. Gao, W. Liu, X. Wang, P. Wang, F. Huang, C. Yao, and Z. Yang. Visual text generation in the wild. In *ECCV*, 2024. 3, 7

TextSSR: Diffusion-based Data Synthesis for Scene Text Recognition

Supplementary Material

6. More Implementation Details

6.1. Model specific settings

In the setup of Sec. 3.2, we consider the specific characteristics of scene text: L is set to 25, and P_M is configured to 128, assuming a background color of 255. It is worth noting that our method is not limited to this configuration. This configuration theoretically enables the generation of text up to 255 characters in length, allowing for background color selection from 255 and character values from 0 to 254. Each character image is set to a 64×64 square, resulting in a character glyph image of size $25 \times 64 \times 64$. The deformed ViT is configured with a patch size of 8, generating a latent feature vector of size 65×1024 , where 1024 represents the dimensionality of the control information required by the CDM.

To meet the rendering requirements for visible characters in the majority of languages, we utilize to employ Puhui Font, an open-source and commercially-free font tool. It adheres to the latest Chinese national standard, GB18030-2022, and supports 178 languages.

6.2. More Details for Datasets

We will further elaborate on the data processing related to training and generation.

Training Data. To train our generative model, we utilize the large-scale multilingual text image dataset, AnyWord-3M [46]. It contains real annotated text boxes and text contents, designed for scene text detection and recognition tasks, which we collectively call AnyWord-Scene. This collection includes a range of popular datasets such as ArT [8], COCO-Text [47], RCTW [41], LSVT [45], MLT [30], MTWI [17], and ReCTS [59]. In addition, two larger datasets are included: Anyword-Wukong [14] and Anyword-Laion [37], which provide a large collection of images with bounding boxes and text content obtained by the PP-OCRv3 [25] detection and recognition model. We filter out anomalous images with pure white backgrounds from the Anyword-3M dataset. Ensuring that when cropping local images, we minimize the inclusion of white borders, thereby reflecting real-world conditions. The processed Anyword-Wukong and Anyword-Laion datasets together contain a total of 3,430,412 complete images, from which we crop 14,856,392 local regions containing text instances for the first training stage. In the second training stage, we utilize 78,395 full images from processed AnyWord-Scene, cropping 201,599 text regions from these.

Data for Accuracy Evaluation. Meanwhile, in Accuracy Evaluation we employ datasets that the model has not

previously encountered. They represent a range of image difficulty levels and cover multiple languages. Specifically, we use the following datasets for evaluation:

- **ICDAR2013** [23]: This benchmark is designed for relatively regular text detection and recognition. We use 233 full images and 917 cropped text images from the test set for evaluation.
- **ICDAR2015** [24]: This dataset contains more challenging real-world scene text, derived from incidental scene captures where the text was not the primary focus. We employ 500 full images and 2,077 cropped text images for evaluation.
- **Shopsign** [57]: This dataset consists of Chinese scene text, primarily from shop signs. We select 183 full images and 932 cropped text images from this dataset.

Base Data for Scalable Generation. We utilize the TextOCR [44], a large-scale scene text dataset including 25,119 images, as the base images for synthetic data generation. To mimic realistic conditions where unlabeled data is abundant, we use pseudo-labels generated by the PP-OCRv3 model, thus simulating a scenario without human annotation.

Generation of TextSSR-F. After the previous step, we obtain 188,526 text regions annotated by the PPOCRv3 model. With the anagram-based method, we expand this data by 8 times, resulting in 1,508,208 synthesized data instances. These are further filtered using the SVTRv2 model, yielding a final dataset of 429,300 fully usable text instances, referred to as TextSSR-F.

6.3. Training and Evaluation Details

We fine-tune our generative model using Stable Diffusion 2.1 (SDv2-1) [36] on eight NVIDIA 3090 GPUs. First, we train the VAE on the full AnyWord dataset with a total batch size of 512 and 256×256 image patches for 150k steps. Then, we freeze the VAE and train the CDM in two stages: 50k steps on AnyWord-Wukong and AnyWord-Laion datasets, followed by 25k steps on the AnyWord-Scene dataset, using a total batch size of 256.

For a fair comparison in our accuracy evaluation, we render all visible bounding boxes and contents annotated in the test datasets. In cases where certain models could not render longer texts or handle multiple text instances per image, we will restrict the input information to within their acceptable ranges, while padding the missing portions. Our model is also limited, with only the first 25 characters rendered for single-character features. For all models, the number of timesteps in the sampling process is set to 20. The evaluation code for generated results is based on the open-source



Figure 8. Visualization results of TextSSR with and without character-level position prior information.

evaluation scripts from Anytext [46] and UDiffText [61]. Except for GlyphControl [53], which requires additional image descriptions to function properly, the other methods only use their predefined text prompts.

In the Realism and extended experiments, CRNN is trained [2] with a batch size of 64 on a single 3090 GPU for 10k steps. Meanwhile, in the Usability experiments, we train three widely-used STR models—CRNN [40], NRTR [39], and ABINet [13]—on the generated data to assess the effectiveness of our synthetic data in enhancing STR performance. All models are trained using the OpenOCR framework, with a total batch size of 1024 on four 3090 GPUs for 100k steps.

The ablation study can be considered a simplified version of the second stage of training, with all settings kept consistent except for the reduction of training steps to 5k. To align with the full-image inference process used in other methods, the image size is set to 512×512 , although training is conducted at a resolution of 256. The “Char-Glyph” ablation experiment involves removing the condition from the CDM training, while the “Char-Position” ablation renders all characters uniformly at a pixel value of 127.

7. Visualization

7.1. Visualization Analysis

Fig. 2 sequentially simulates various situations, including English text in a regular scene, text under challenging conditions, and Chinese text in a natural setting. TextSSR consistently generates accurate and high-quality visual text, demonstrating several powerful capabilities: (1) it can synthesize arbitrary text with standard glyphs from any language, as shown in examples of both Chinese and English; (2) it learns font style information from surrounding context, such as the font color in Sample 1, which is derived from the horizontal line below; (3) it synthesizes correct text even without strong background information, as illustrated in Sample 2, where the local image provides no usable in-

formation for imitation; and (4) it exhibits scale invariance, allowing for text synthesis in scenes of any size, with the three samples representing large, small, and medium text sizes, respectively.

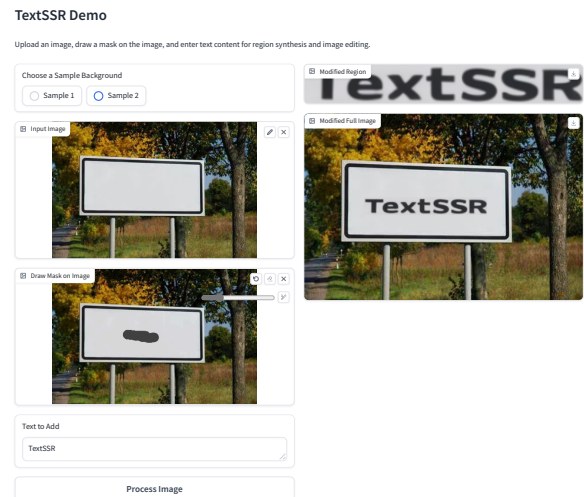


Figure 9. Users will select a scene image as the base, perform mask marking in the designated area, and then input the text content to be written. After processing, the desired text region and the edited original image will be obtained.

7.2. Function Demonstration Platform

We have concretely implemented the inference process and build a demonstration demo. To ensure that the user input matches the label format used during training, we recalculate text boxes that align with the input text layout after the user applies the mask. As shown in Fig. 9, the text is roughly displayed within the user-specified area, though it does not follow the mask strictly.



Figure 10. Visualization results of TextSSR with and without character-level glyph prior information.

7.3. Ablation Visualization Results

Fig. 8 and Fig. 10 illustrate the impact of character-level position and glyph on the rendering results of TextSSR. The results indicate that omitting either component leads to issues such as character deformation, incorrect characters, and duplication errors in some cases, further supporting the findings of the ablation study.

7.4. More Visualization Results

To provide a detailed illustration of the synthesis process and effectiveness of TextSSR, Fig. 11 demonstrates how TextSSR utilizes the region from the original image to reconstruct a local image, which is then further cropped to obtain the desired result. A comparison with the ground truth is also shown, highlighting the strong synthesis capabilities of TextSSR.

7.5. Failure Cases

It is important to note that our synthesis method is not flawless and has certain limitations. Fig. 12 presents several common failure cases, which can be attributed to the following reasons:

1. **Long text:** Excessively long text can confuse the model, resulting in disordered text images. This issue is exacerbated by the limited amount of training data for such cases.
2. **Blurred regions:** When the text region itself is excessively blurred, the model struggles to accurately reconstruct and synthesize the text.
3. **Multi-directional text:** The model, primarily trained on horizontally aligned text, faces challenges with multi-directional text, especially vertical text. Applying rotation-based post-processing, as used in STR methods, could be a potential solution.
4. **Incorrect text labels:** Errors in manual labeling can lead to mismatches between the rendered regions and their corresponding labels.

5. **Language Characteristics:** The performance on Chinese text is generally worse than on English, due to the higher number of characters and the complexity of Chinese characters.

8. Discussion

However, our study has limitations and avenues for further research, including the following: (1) The text layout and the text content must be paired. While we utilize the anagram-based method to mitigate this issue, we will design methods for reasonable, large-scale usable pairings for broader synthesis considerations. (2) Currently, large-scale synthetic post-processing relies on an STR model; we aim to integrate a self-checking mechanism into the entire framework to verify the correctness of the synthesized output. This could further enhance learning and adjust the arrangement of text layout until generating usable text correctly. (3) Due to available large-scale scene text images already used for training, we plan to collect a larger dataset of untrained text images for the base images, creating a more extensive synthetic dataset to benefit the STR community.

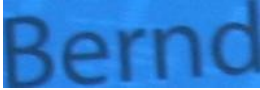
| Scene Text Image | Scene Text Region | TextSSR Output | TextSSR Region |
|------------------|--|----------------|----------------|
| | <p data-bbox="607 262 750 289">Text Content</p>  <p data-bbox="634 422 732 449">Bernd</p> | | |
| |  <p data-bbox="607 640 760 667">Summer's</p> | | |
| |  <p data-bbox="646 884 721 911">LINK</p> | | |
| |  <p data-bbox="646 1106 721 1134">Care</p> | | |
| |  <p data-bbox="646 1287 721 1314">手套</p> | | |
| |  <p data-bbox="555 1493 812 1528">13333851288</p> | | |
| |  <p data-bbox="548 1724 818 1759">A2区11排623号</p> | | |

Figure 11. More visualization results for TextSSR.

| Scene Text Image | Scene Text Region | TextSSR Output | TextSSR Region |
|------------------|--|----------------|----------------|
| | <p data-bbox="583 541 743 569">Text Content</p> <p data-bbox="526 632 813 680">Informatikforschung</p> | | |
| | <p data-bbox="553 1035 769 1077">(Builders)</p> | | |
| | | | |
| | <p data-bbox="630 1318 716 1352">Talk</p> <p data-bbox="526 1398 813 1457">电话: 18238451063</p> <p data-bbox="526 1493 813 1535">绰18238451063</p> | | |

Figure 12. Failure Cases. We show several disappointing synthesis results produced by TextSSR.